A Primitive Equations Model Study of the Effect of Topography on the Summer Circulation over Tropical South America

ADILSON W. GANDU* AND JOHN E. GEISLER

Department of Meteorology, University of Utah, Salt Lake City, Utah

(Manuscript received 12 February 1990, in final form 9 January 1991)

ABSTRACT

A nonlinear, primitive equations model with five levels in a σ coordinate is applied to study the effects of idealized topography on the summer circulation pattern over tropical South America. The model circulation is forced by prescribed latent heating centered over the Amazon Basin. Both the steady and the transient components of the response are considered and compared with the corresponding components in the absence of topography. It is found that topography blocks low-level inflow from the equatorial Pacific and leads to the development of a steady, northerly jet that is fed from the tropical Atlantic. Other important effects of topography on the response to steady heating are found in the low-level field of vertical motion. The effects of topography on the response to transient heating are described in terms of a component reflected to the east and a component transmitted to the west by the topography.

1. Introduction

The atmospheric circulation pattern over tropical South America has received increased attention in recent years as a result of a growing awareness of the potential impacts of tropical deforestation upon it. The hypothesis is that changes in surface fluxes of heat and moisture consequent to deforestation of the Amazon Basin would lead to a significant decrease in the level of convective activity in the summer rainy season. This would alter the circulation pattern, which is presumed to be driven by the latent heat release associated with the convection. Recent advances in the parameterization of the effects of vegetation and soil properties on surface fluxes (Dickinson 1984; Sellers et al. 1986) have opened the way toward model testing of this hypothesis. Incorporation of these surface parameterizations into general circulation models has resulted in quantitative estimates of the impact of the deforestation on the circulation and other aspects of the local climate of tropical South America (Dickinson and Henderson-Sellers 1988; Nobre et al. 1989).

A better understanding of how the circulation pattern over tropical South America varies with the level of convective heating would help in the interpretation of impact studies using general circulation models coupled to detailed parameterizations of surface processes. A recent study by Horel et al. (1989) documented the annual cycle of convective activity and circulation patterns over the tropical Americas using current large-scale datasets, but did not produce any new insight into the dynamical link between convective activity and the summertime circulation pattern over tropical South America. The largest contribution to present understanding of the dynamics of this circulation has come from studies using relatively simple models. Yet, until very recently, none of these models made any attempt to deal with the topography that uniquely characterizes this region of the tropics. The purpose of this paper is to present the results of a study of the response to prescribed large-scale convective heating in a relatively simple model that includes topography representative of the region. The remainder of this introduction is devoted to a review of past modeling studies of this type.

The dominant feature of the upper-level summertime circulation over tropical South America is a large anticyclone, often referred to as the Bolivian high, whose climatological center is over the Bolivian Altiplano (Kreuels et al. 1975; Virji 1981). The situation is much different at low levels, where the flow crosses the northeast coast of South America from a general northeasterly direction, then moves poleward parallel to the Andes. The size and position of the Bolivian high bears close resemblance to the response of the linear model of Gill (1980) to a heat source located close to the equator. The first application of the Gill type of model to the circulation over tropical South

* Visiting Scientist from Departmento de Meteorologia, Universidade de São Paulo, Brazil.

Corresponding author address: Dr. J. Geisler, Dept. of Meteorology, University of Utah, 819 William C. Browning Bldg., Salt Lake City, UT 84112-1183.

America was that of Silva Dias et al. (1983). The main interest in that study was the response to transient bursts of convection, ranging from the diurnal cycle to fluctuations on the time scale of a few days, and the prescribed heating was therefore smoothly switched on at some initial time and subsequently switched off again. A feature closely resembling the observed Bolivian high appeared at upper levels, together with a large-amplitude transient that traveled eastward out of the model domain. A distinguishing feature of this model was the use of an expansion in terms of normal modes to solve the model equations. This technique lent itself naturally to an interpretation of the transient response in terms of propagating normal modes.

The analysis of the transient response to prescribed heating by Silva Dias et al. (1983) was extended to the steady-state response in a model study by DeMaria (1985). This model constituted an advancement over the single-vertical-mode models of Gill (1980) and Silva Dias et al. (1983), insofar as it contained five vertical modes. The steady flow pattern in this model at low levels bore little resemblance to the observed summer climatology. In particular, the unrealistic low-level flow from the west, across the region where the Andes would be and into the heat source, highlighted the need for incorporation of the topography into such models. A further feature of the DeMaria (1985) study was its description of the patterns of vertical motion associated with the steady response and the transient response. The vertical motion patterns associated with the transient response were also examined in a study by Buchmann et al. (1986), which employed a two-layer, nonlinear model. In common with all previous studies, that model contained no topography.

A first step in the investigation of the response to prescribed heating over tropical South America in the presence of topography was taken by Kleeman (1989). Topography in the two-layer model used in that study was represented by a meridionally oriented "knife-edge" filling the bottom layer. The study was restricted to an analysis of the transient response over a three-day period. A distinguishing feature of the model was an analysis in terms of analytic solutions that facilitated an interpretation of transient patterns in terms of normal modes reflected and transmitted by the topographic barrier. The development of a Bolivian high in the upper layer of the model was shown to be little affected by the presence of the topographic barrier, while the circulation pattern in the lower layer exhibited an inflow from the equatorial Atlantic side of the domain that funneled into a jet directed southward along the barrier.

The model used in the study presented in this paper is a nonlinear, primitive-equations, gridpoint model with five levels in the vertical. Topography is represented by a meridionally oriented ridge of Gaussian cross section. A prescribed heat source to the east of the topography is turned on smoothly and maintained to provide the steady-state response that is the principal object of study in this paper. The features of this response are compared with those resulting from the same simulation in the absence of topography. The circulation patterns in this no-topography control run differ slightly from those in the DeMaria (1985) study because of nonlinear effects and the use of a different basic-state temperature profile. Simulations with a transient heat source and various forms of idealized topography are also presented and compared with the results of the Kleeman (1989) study.

2. The model

The model employs the nonlinear, primitive equations in spherical coordinates. The vertical coordinate is $\sigma = (p - p_T)/(p_S - p_T)$ where $p_T = 50$ mb and $p_S = 1000$ mb. There are five levels in the vertical, with the variables distributed as indicated in Fig. 1. Horizontal finite differencing in the model conforms to the C grid of Arakawa and Lamb (1977). The gridpoint spacing is 3.75° in both longitude and latitude. There is no horizontal or vertical diffusion in the model, dissipation being parameterized in the form of Rayleigh friction and Newtonian cooling with a common rate constant of 5 day^{-1}. The model contains a standard routine for interpolation of fields from σ surfaces to p surfaces.

The horizontal domain of the model is shown in Fig. 2. Rigid vertical walls are imposed at 45°N and 60°S. At the eastern and western boundaries, the radiation condition of Orlansky (1976) is imposed. Also

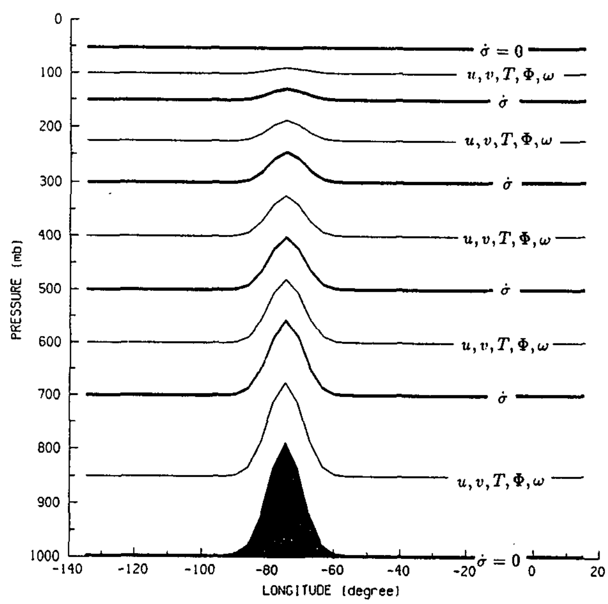

FIG. 1. Longitudinal cross section illustrating the vertical distribution of the σ levels on which the model variables are evaluated. The topography is that given in Fig. 2. Away from the topography the surface pressure is 1000 mb.

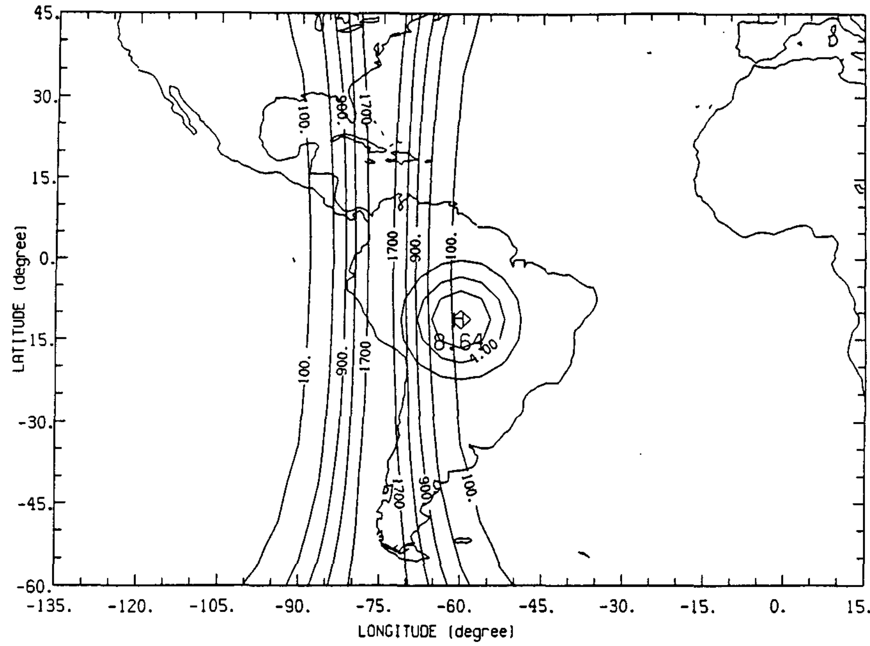

FIG. 2. The horizontal domain of the model. Circular contours represent the heating rate (K d^{-1}) at 400 mb. Contours oriented meridionally represent the topography, which has a Gaussian cross section of scale 800 km and maximum height 2 km. The distortion of the height contours is a consequence of the cylindrical map projection.

shown in Fig. 2 are contours of the topography and contours of the prescribed heating at the level where it is a maximum. The heating is centered off the equator in the region of the observed maximum of convective activity in the summer. The vertical structure of the heating follows the prescription of DeMaria (1985), which is a slightly skewed parabola with a maximum at 400 mb.

In this study we consider the response to the two different temporal variations of heating that are shown in Fig. 3. One is a steady heat source that is turned on gradually to minimize the transient component of the response. The other source peaks sharply and then decays to zero and is the heat source that was used by DeMaria (1985) and by Kleeman (1989) to excite a transient response. In the present study it has been normalized such that the total heat supplied is equal to that delivered by the steady heating over a period of 72 hours.

In the case of both the steady heating and the transient heating experiments, the initial state is one of rest, except in the one experiment in which a basic-state flow from the west is imposed. The basic-state static stability is given by the temperature distribution $T = T_S(p/p_S)^\Gamma$ where $T_S = 300$ K, $p_S = 1000$ mb, and $\Gamma = 0.19$. In the at-rest basic state, the presence of topography gives rise to a motion field even in the absence of the prescribed heating, but this field is small and has no discernible effect on the pattern of the response represented as an anomaly relative to a horizontally uniform basic state of rest. In the simulations with the slowly rising steady forcing, the amplitude of the transients are sufficiently small that a temporal av-

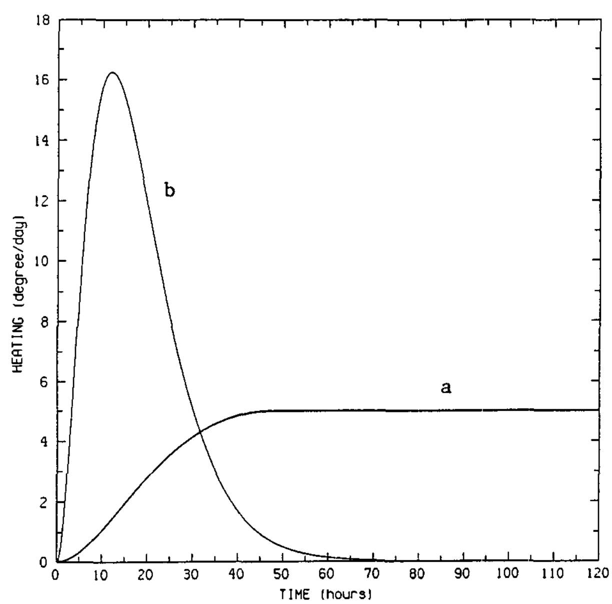

FIG. 3. The temporal dependence of the prescribed heating used in (a) the steady-state simulations and (b) the transient simulations. The units of the ordinate are the vertically integrated heating rate in kelvins per day.

erage was not needed to isolate the steady response. We take the solution at $t = 120$ hours as representative of the steady response.

3. The steady-state response

The basic features characteristic of the steady-state response when there is no topography present in the model are illustrated by the three panels of Fig. 4. In this and succeeding figures, continental outlines are shown to give an impression of scale. At the 200 mb level the circulation is dominated by the simulated Bolivian high. In the eastern part of the domain the response has the characteristics of a stationary Kelvin wave packet, symmetric with respect to the equator and decaying away from the source region. At the 850 mb level, the circulation pattern closely resembles the 200 mb pattern, but with opposite sign. The 500 mb vertical motion field exhibits a pattern of upward motion that coincides with the imposed heating. The principal region of compensating subsidence is found slightly south of west of the heating region. There is a secondary region of subsidence along the equator to the east of the heating.

For the purpose of generating a solution of the linearized equations for comparison, we reduced the heating by a factor of ten, repeated the simulation, and then scaled the response up by the same factor. This solution (not shown) was in close agreement with that obtained by DeMaria (1985). The features exhibited by the linear response relative to the nonlinear response (Fig. 4) consisted of a modest increase in the amplitude of the circulation at both upper and lower levels and a decrease in the turning radius of the outflow pattern at upper levels. Associated with the latter effect was a small reduction in the amplitude of the trough that appears to the northeast of the simulated Bolivian high in Fig. 4a.

A two-dimensional ridge of topography of maximum height 2 km (Fig. 2) was then inserted into the model and the simulation with the steady heating was repeated. The 200 mb circulation pattern that resulted closely resembled that in Fig. 4a and is not shown here. The circulation pattern at low levels was much altered by the insertion of topography. Figure 5a shows the circulation pattern on the lowest σ surface ($\sigma = .842$). Interpolation onto the 850 mb surface, assuming that horizontal velocity vanishes at the ground, yields the circulation pattern shown in Fig. 5b. The strip of 850 mb surface that is below the topography is indicated by the absence of wind vectors. Figure 5b is to be compared with Fig. 4b. It is seen that at this level the topography blocks the flow that previously came from the Pacific. The low-level inflow now has its roots on the Atlantic side in a broad region symmetric with respect to the equator. This flow subsequently feeds into a jet that crosses the equator, moves through the heat source region (centered at 60°W, 11°S), and then turns sharply north to weaken and move along the eastern slope of the topography. A cross section of the jet at the equator is shown in Fig. 5c. The topography roughly occupies the region centered at 75°W, which is enclosed by the zero contour. As noted previously, there is no diffusion acting in the model; and the contours on the side of the jet facing the topography are closed by the assumption, made within the routine that interpolates to p surfaces, that the horizontal velocity is zero at the ground.

The presence of topography does not alter much the 500 mb vertical velocity pattern that was shown in Fig. 4c, so that the changes can be described without the aid of a figure. What results is a reduction in the areal extent of the subsidence pattern to the west of the heat source that is compensated by an increase both in areal extent and peak value (from 3.3 to 5.4 mb day^{-1}) of the subsidence pattern along the equator to the east of the heat source. At low levels, on the other hand, the changes in vertical motion brought about by the topography are considerable. We describe these with the aid of Fig. 6.

The field of vertical motion at the 850 mb level when there is no topography present is shown in Fig. 6a. This is to be compared with Fig. 6b, which shows vertical motion at the same level in the simulation with topography present. It can be seen that the addition of topography introduces two regions of relatively strong subsidence near the equator. The region to the east of the longitude of the heat source, considered jointly with the low-level flow that was shown in Fig. 5b, suggests that the topography has set up a circulation cell in the equatorial plane that constitutes a feed for the low-level jet that flows southward into the region of the heat source. The model predicts that the zonal scale of this circulation is quite small, with the center of the low-level subsidence falling very close to the northeast coast of South America. Figure 6b also reveals the existence of a concentrated region of subsidence to the west of the longitude of the heat source. The small scale of this feature is partly dictated by the fact that the 850 mb surface on which it is depicted passes beneath the topography at the location of the meridionally oriented zero contour in the height field. To make this point clearer, we show in Fig. 6c the vertical motion pattern as it appears on the lowest σ surface. This shows that the region of subsidence is of somewhat larger extent and is also somewhat stronger than is indicated in Fig. 6b. We defer further discussion of this feature until the concluding section.

We have modified the model to include a westerly basic-state flow that is uniform in longitude and increases linearly in σ from a value of zero at the surface to a value of 10 m s^{-1} at $\sigma = 0.15$. The steady response patterns in the presence of this basic-state flow are illustrated in Fig. 7. The top panel (Fig. 7a) shows the low-level response ($\sigma = 0.842$) in the absence of the Amazon Basin heating. The topography that has been

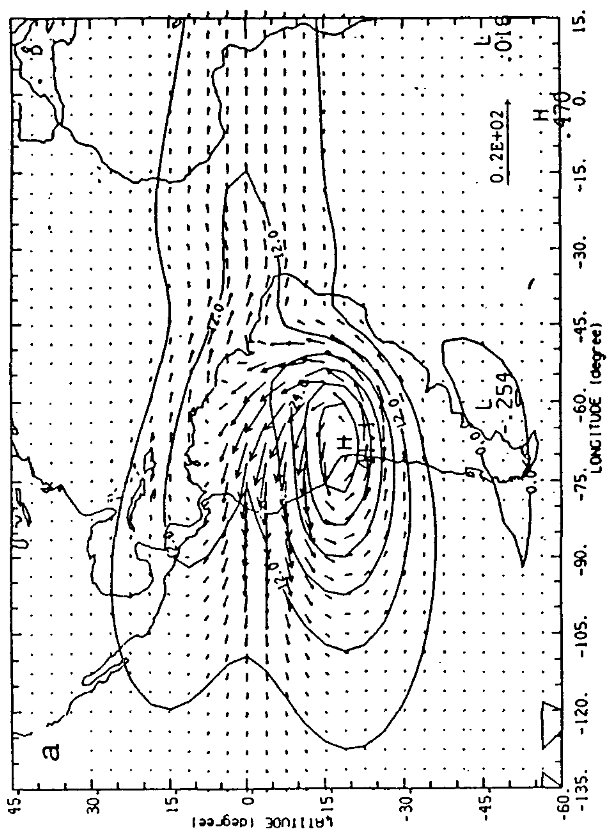

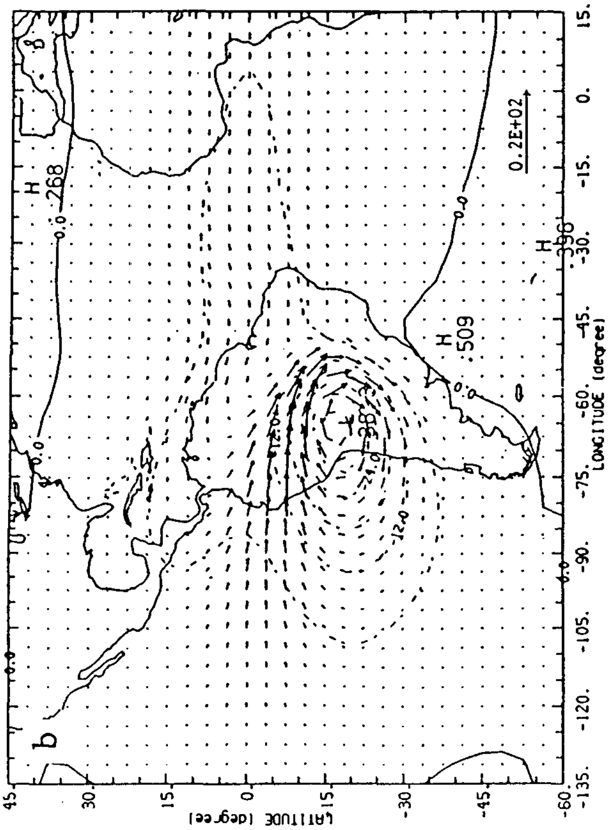

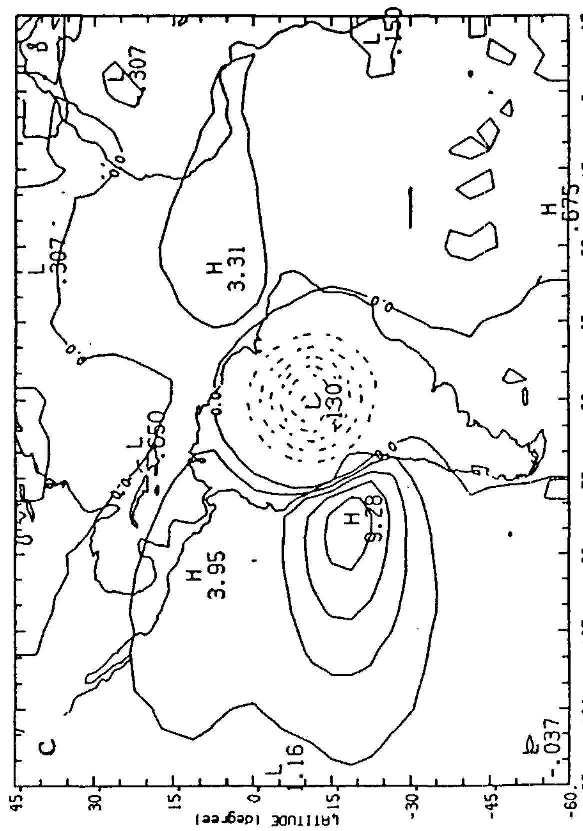

FIG. 4. The steady-state response in the absence of topography as illustrated by (a) 200-mb height and vector wind, (b) 850-mb height and vector wind (c), 500-mb vertical motion, ω. In this and succeeding figures, the height field is an anomaly relative to the horizontally uniform height field of the basic state. Contour interval of height is 6 m. The vector shown in lower right-hand corner of (a) and (b) represents 20 m s^{-1}. Contour interval of vertical motion is 20 mb d^{-1} when $\omega < 0$ and 2 mb d^{-1} when $\omega > 0$.

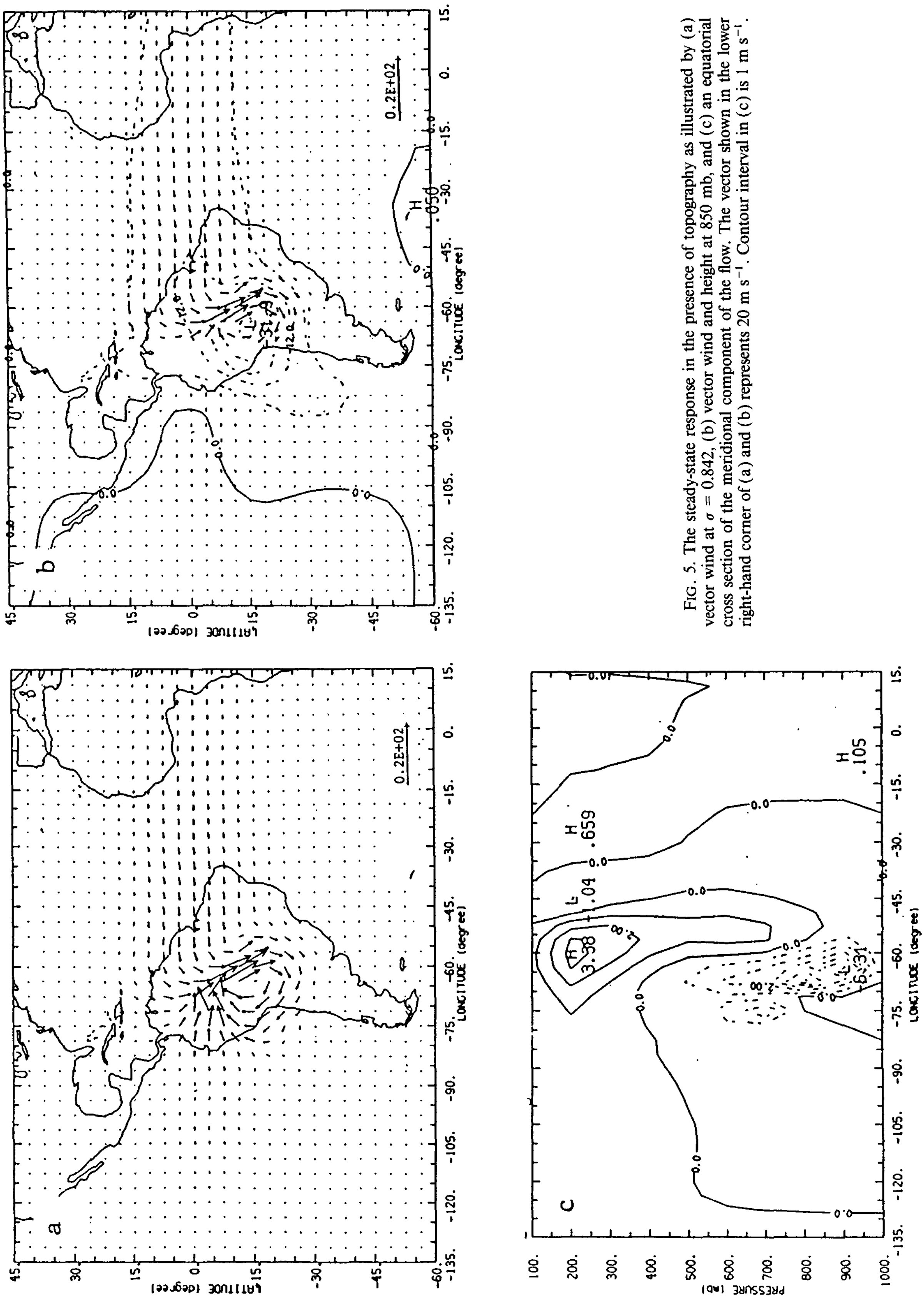

FIG. 5. The steady-state response in the presence of topography as illustrated by (a) vector wind at $\sigma = 0.842$, (b) vector wind and height at 850 mb, and (c) an equatorial cross section of the meridional component of the flow. The vector shown in the lower right-hand corner of (a) and (b) represents 20 m s^{-1}. Contour interval in (c) is 1 m s^{-1}.

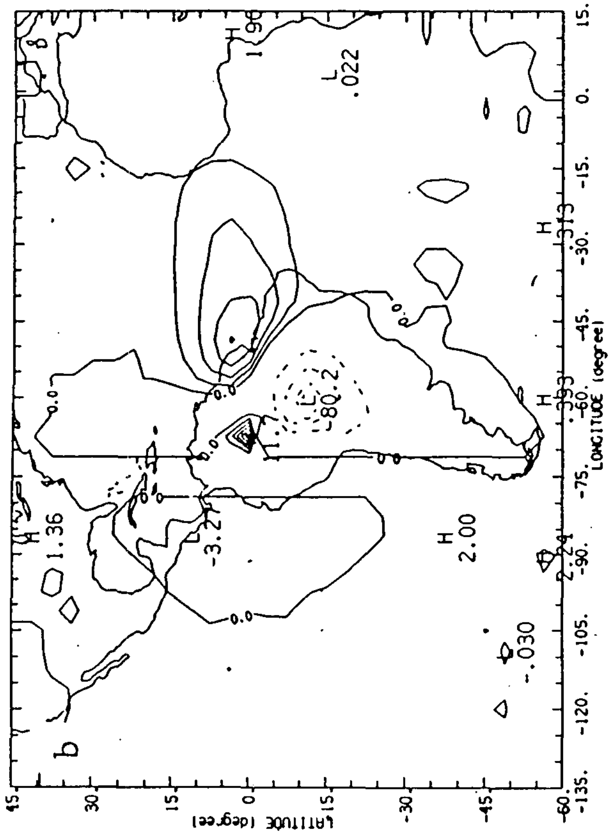

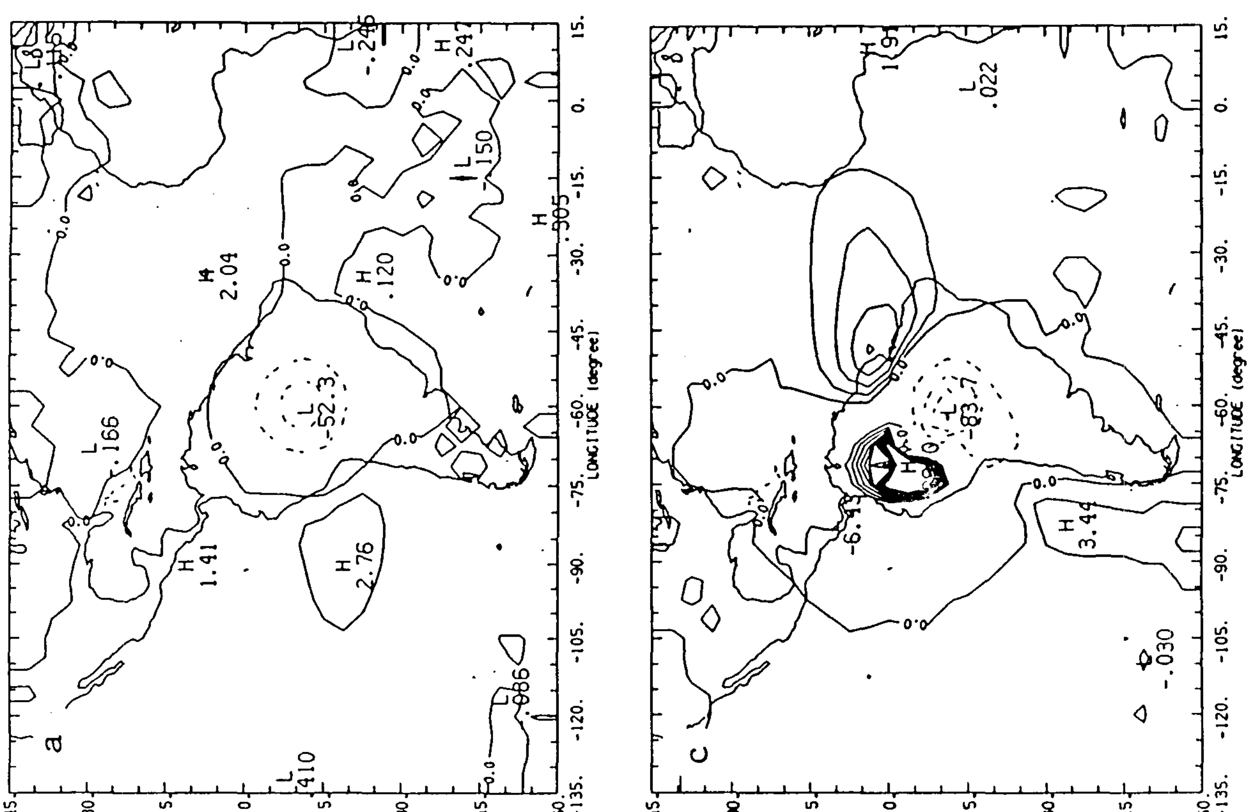

FIG. 6. (a) The steady-state pattern of vertical motion (ω) at 850 mb in the absence of topography; (b) same as (a), but in the presence of topography; and (c) same as (b), but on the surface $\sigma = 0.842$. Contour interval is 20 mb d^{-1} when $\omega < 0$ and 2 mb d^{-1} when $\omega > 0$.

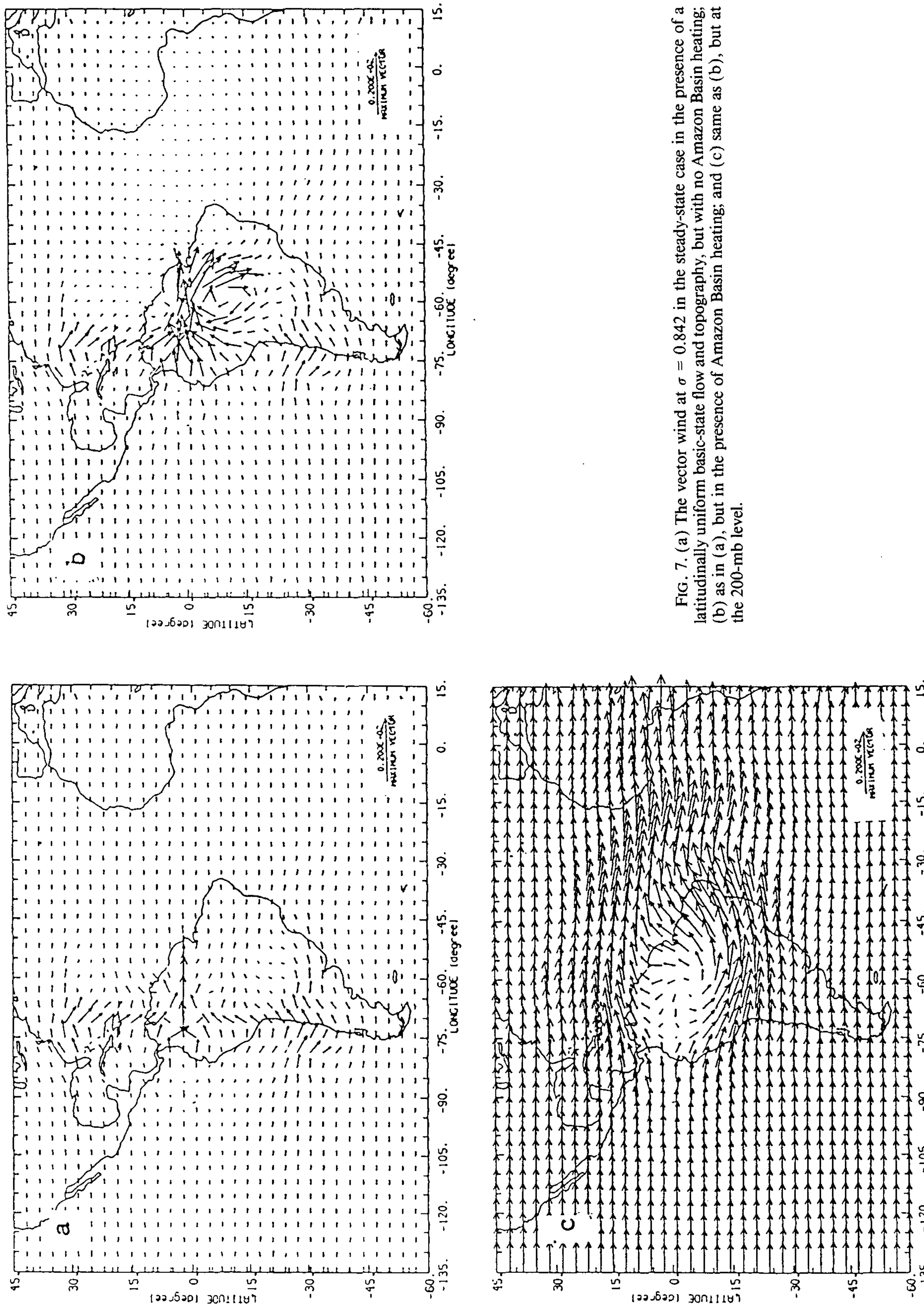

FIG. 7. (a) The vector wind at $\sigma = 0.842$ in the steady-state case in the presence of a latitudinally uniform basic-state flow and topography, but with no Amazon Basin heating; (b) as in (a), but in the presence of Amazon Basin heating; and (c) same as (b), but at the 200-mb level.

used in the simulations described so far in this paper (Fig. 2) has here been tapered in latitude so that it falls to zero before reaching the northern and southern boundaries of the model. Thus, at high southern latitudes in Fig. 7a the flow is zonal. At somewhat lower latitudes ($\sim$35°S) there is a tendency for the flow to go around the southern flank of the tapered ridge, while in subtropical latitudes ($\sim$15°S) the flow is over the ridge. The regions of relative vorticity successively entered by a parcel crossing over the ridge in subtropical latitudes in Fig. 7a (weak cyclonic, strong anticyclonic, weak cyclonic) conform to the description of quasi-geostrophic flow over a mountain given by Smith (1979). In a narrow strip centered on the equator the flow pattern becomes more complicated, the most significant feature being an enhancement of the westerly flow that extends a considerable distance downstream of the ridge.

The low-level response in the presence of the basic-state flow and Amazon Basin heating is shown in Fig. 7b. The circulation pattern here is largely a superposition of the pattern in Fig. 7a and the pattern in Fig. 5a. It is clear from Fig. 7b that even the relatively weak basic-state flow of 1.5 m s^{-1} at this level is sufficient to shut off the inflow of air from the tropical Atlantic into the cyclonic circulation over the Amazon Basin. Finally, Fig. 7c shows the circulation pattern at the 200 mb level. This figure should be compared with Fig. 4a, which characterizes the response in the absence of the basic-state flow. It can be seen that the inclusion of the basic-state flow adds considerable definition to the trough located downstream of the simulated Bolivian high.

4. The transient response

In this section we describe the results of simulations in which the heating, as shown by the large-amplitude curve in Fig. 3, rises sharply to a maximum in 12 hours and then decays exponentially. As remarked earlier, this heat source is identical to that used in the no-topography model simulations by Silva Dias et al. (1983) and DeMaria (1985) and in the simulation with topography present described by Kleeman (1989).

Figure 8 illustrates the evolution of the transient response at the 200 mb level in the case where no topography is present in the model. The pattern at the 850 mb level (not shown) is of the same form, but with the sign reversed. It can be seen that the concentrated local response at 20 hours separates by 36 hours into a large-amplitude Kelvin wave packet and a circulation to the west of the longitude of the heat source that closely resembles the simulated Bolivian high in the steady-state case (Fig. 4a). The Kelvin wave packet then propagates out of the domain, indicating that the radiation boundary condition in the model functions well in this application. The transient Bolivian high subsequently decays at a rate that is governed by the dissipation in the model. Comparison of the patterns in Fig. 8 with corresponding ones in Silva Dias et al. (1983) and in DeMaria (1985) reveals that the nonlinear nature of the present model adds nothing of significance to the evolution of the transient response pattern in the absence of topography.

Topography in the two-layer model simulation of the transient response described by Kleeman (1989) was represented by a meridionally oriented knife-edge filling the lower layer. We first consider the response in our model to this very idealized topography, which we represent by imposing a boundary condition of zero zonal flow along 75°W in a layer 4 km deep. We represent the result in the form of a time series of maps showing the difference obtained by subtracting the simulation with no topography from the simulation with topography. Figure 9 shows such a sequence for the transient response at 200 mb. The eastward traveling Kelvin wave packet seen there is, by definition, the component of the transient solution that is reflected from the topographic barrier. This reflected component has the same structure and comparable amplitude, but opposite sign, at low levels. Also evident in Fig. 9 is a broad and relatively slow-moving anticyclonic transient in the western part of the domain. Reference to the corresponding difference map at the 850-mb level (not shown) reveals that this transient to the west of the topography is essentially barotropic.

Both of the aforementioned components of the transient solution appeared in the simulation by Kleeman (1989), who referred to them as the reflected and the transmitted components, respectively. These two components also appear in those simulations with our model in which the topography is represented more smoothly as a meridional ridge of Gaussian cross section and lower altitude. We proceed now to describe these two components in more detail. In the interests of economy of presentation, we take as an index of the amplitude of Kelvin wave transients the zonal wind at a point located at 45°W and the equator. For reference, we show first in Fig. 10a the time series for 200 mb and 850 mb zonal wind at this geographical point in the simulation with no topography. This is the Kelvin wave packet that is launched directly by the transient heating, and whose spatial dependence was illustrated in plan view in Fig. 8. It can be seen from Fig. 10a that the vertical structure is essentially that of an internal normal mode with a node in the middle troposphere. Figure 10b shows the time series of zonal wind differences obtained by subtracting the no-topography simulation from the simulation in which topography is represented by the knife edge of 4 km altitude. This is the reflected Kelvin wave packet previously seen in plan view in Fig. 9. Both the basic low frequency packet and a superimposed higher frequency modulation exhibit the same vertical structure that characterizes the transient coming directly from the heat source (Fig. 10a). When the knife-edge topography in the model

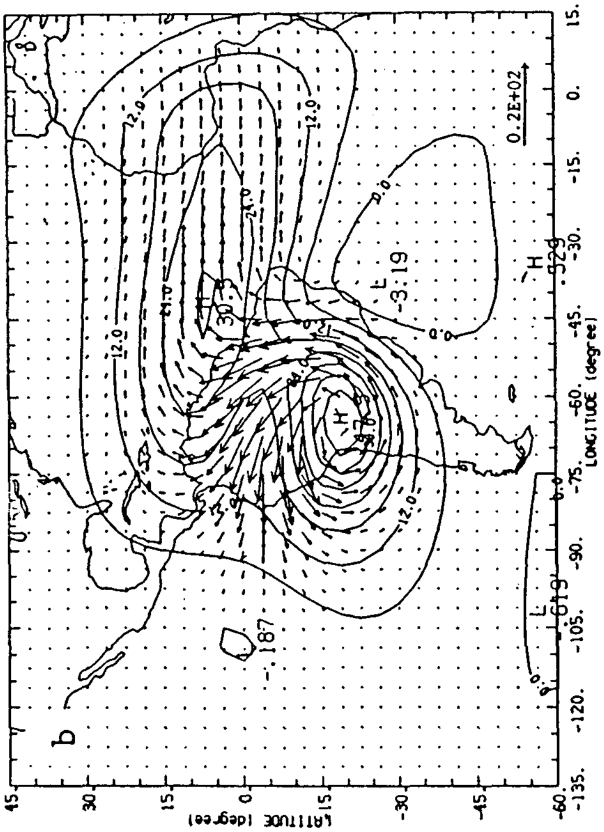

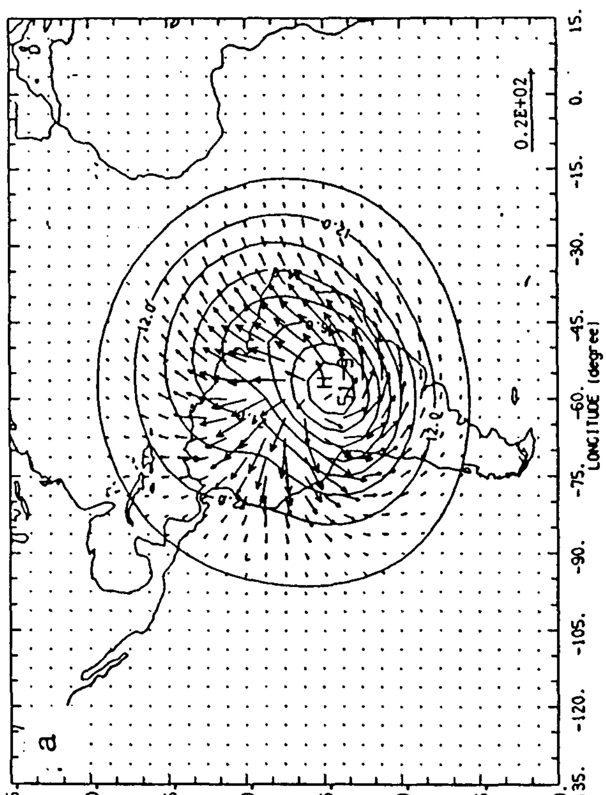

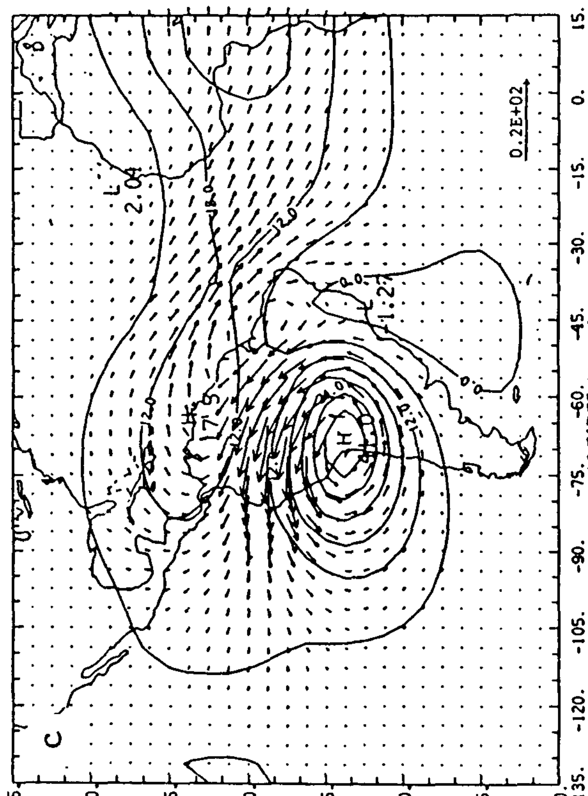

FIG. 8. The response to transient heating in the absence of topography as represented by 200 mb height and vector wind at (a) $t = 20$ h, (b) $t = 36$ h, and (c) $t = 48$ h. Contour interval of height is 6 m; the vector shown in the lower right-hand corner represents 20 m s^{-1}.

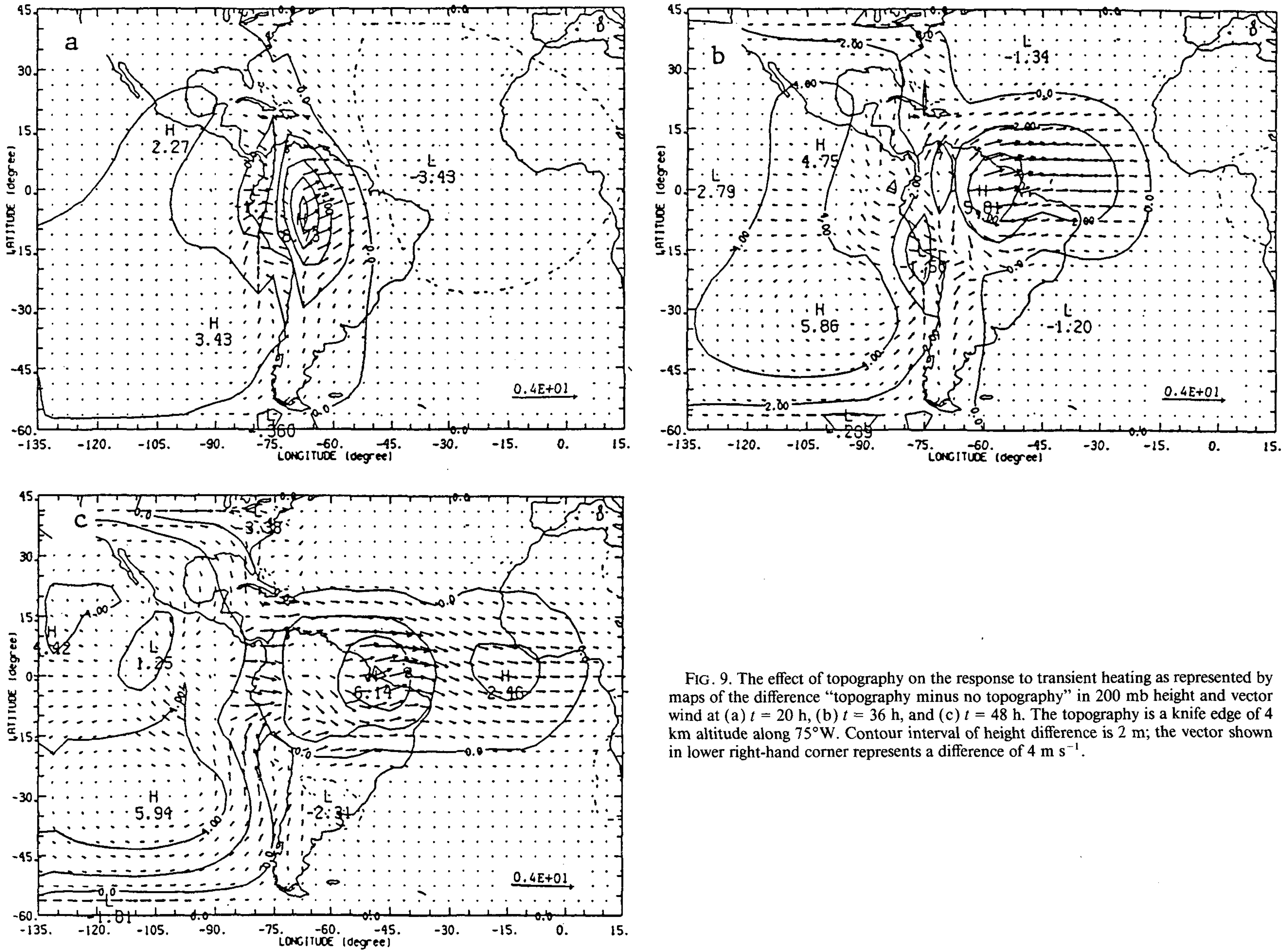

FIG. 9. The effect of topography on the response to transient heating as represented by maps of the difference "topography minus no topography" in 200 mb height and vector wind at (a) t = 20 h, (b) t = 36 h, and (c) t = 48 h. The topography is a knife edge of 4 km altitude along 75°W. Contour interval of height difference is 2 m; the vector shown in lower right-hand corner represents a difference of 4 m s^{-1}.

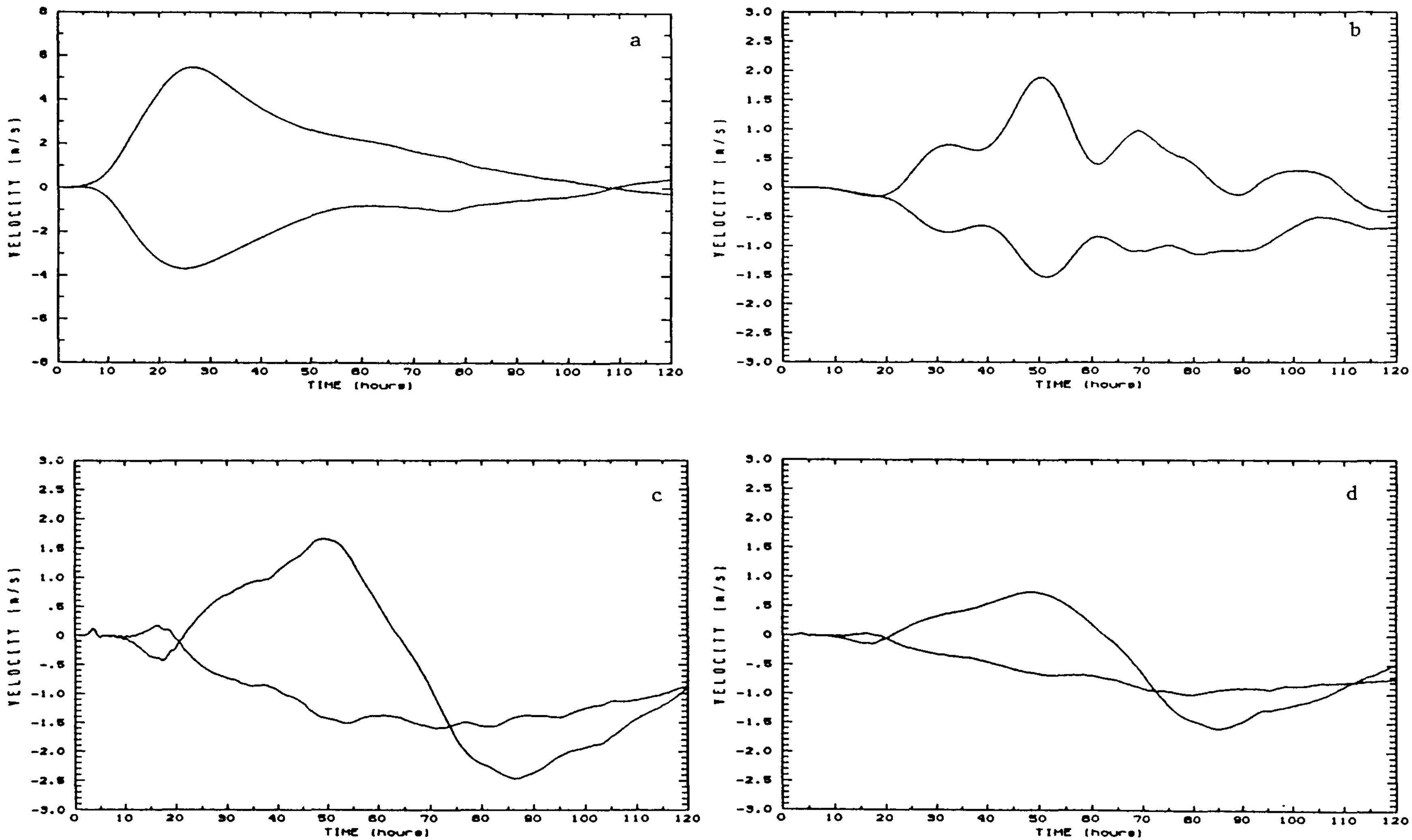

FIG. 10. (a) Zonal component of wind at the point 0°, 45°W at 200 mb (upper curve) and at 850 mb (lower curve) in the transient heating case with no topography; (b) as in (a), but for the difference "topography minus no-topography" when the topography is a knife edge of 4 km altitude along 75°W; (c) same as (b), but for Gaussian topography of scale 800 km and maximum altitude of 4 km; and (d) same as (c), but for maximum altitude of 2 km. Note that the scale of the ordinate in (a) differs from the scale in the other three frames of the figure.

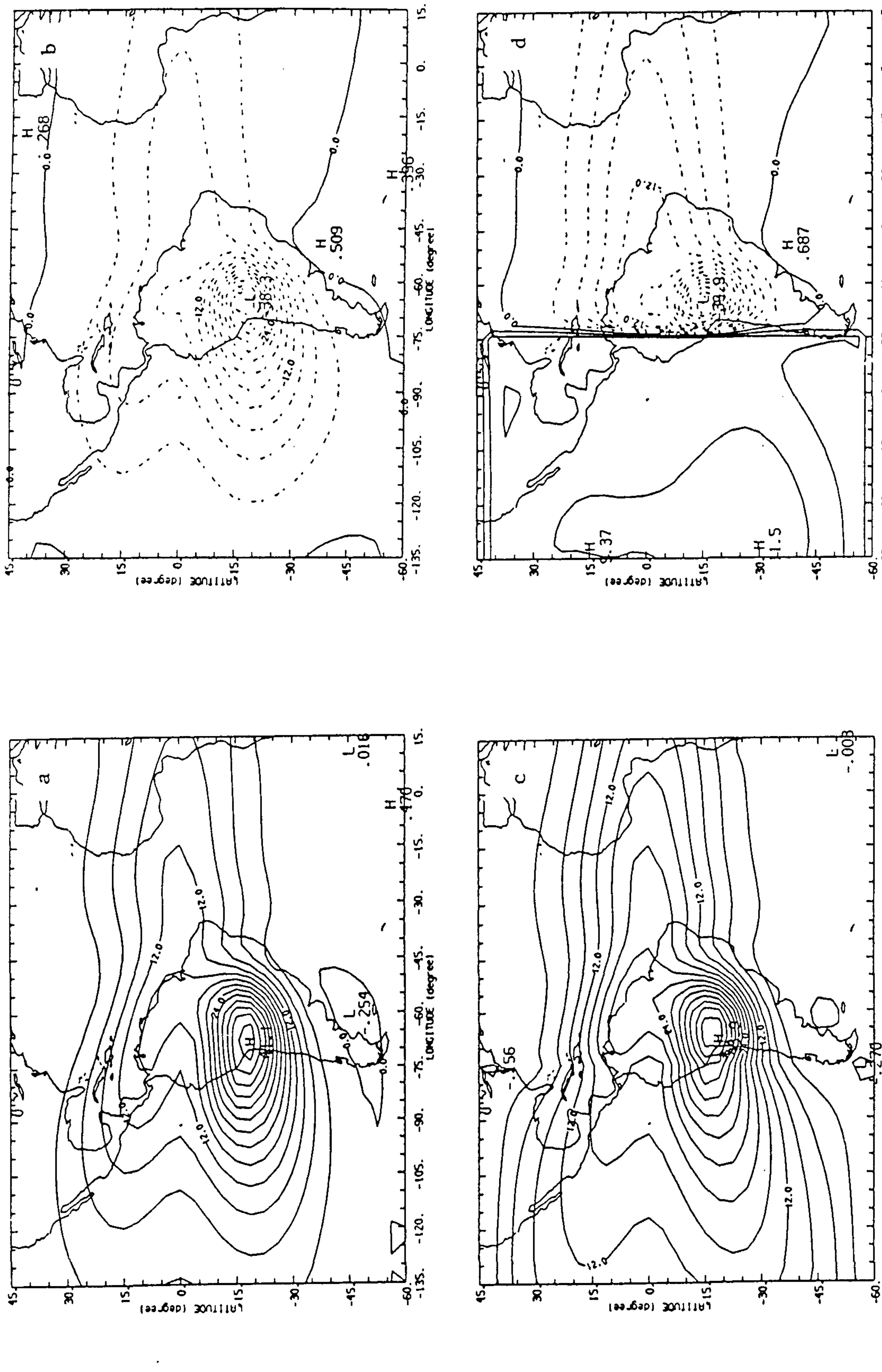

FIG. 11. (a) Steady-state 200-mb height field (anomaly relative to the basic state) in the absence of topography; (b) same as (a), but for 850 mb; (c) same as (a) but for the case with knife-edge topography of altitude 4 km; and (d) as in (c), but for 850 mb. The contour interval in all cases is 3 m.

is replaced by Gaussian topography of the same altitude (4 km) and Gaussian width scale of 800 km, the reflected Kelvin wave packet appears as in Fig. 10c. The amplitude remains about the same as it was in Fig. 10b, but the high frequency component has been eliminated and the vertical structure cannot now be described as a single vertical normal mode with a node in the middle troposphere. In a simulation with the amplitude of the Gaussian ridge topography reduced to 2 km, the reflected Kelvin wave packet behaves as in Fig. 10d. This looks like the case in Fig. 10c, but with amplitude reduced by a factor of two.

We consider now the transmitted component of the transient response, which is found to the west of the topography. Kleeman (1989) remarked on its essentially barotropic structure and was of the opinion that a study by Silva Dias and Bonatti (1985) provides some observational confirmation of its existence. These authors performed a vertical normal mode decomposition of the time-mean flow in the region of South America, defined as the average of FGGE level IIIb data for the period 29 January to 16 February 1979. They then displayed the part of this flow pattern accounted for by the external normal mode alone. The external-mode flow pattern was relatively weak everywhere except for an anticyclonic circulation centered over the southeast Pacific at about 20°S, 100°W, which is in the neighborhood of the southeastern Pacific center of the transmitted transient component shown in Fig. 9. It is this qualitative agreement with the transient component that prompted Kleeman (1989) to cite the Silva Dias and Bonatti (1985) study. Since their analysis was performed on a 3-week average, we feel that it is more appropriate to compare their result with the steady response rather than the transient response. The steady response in the presence of knife-edge topography of 4 km is shown in Figs. 11c and 11d. The response in the absence of topography is shown for comparison in Figs. 11a and 11b. It is clear that the effect of topography on the response over the eastern Pacific is an enhancement of the height field that is characterized by a relatively strong barotropic component. Estimating the amplitude of the external-mode contribution to this response by taking the two-point vertical average, we arrive at a figure of about 10 m for the amplitude in a broad area around 20°S, 100°W. This is about half of the amplitude obtained by Silva Dias and Bonatti (1985).

5. Summary and discussion

In this study we have employed a fully nonlinear, primitive equations model to isolate the effect of an idealized Andes mountain chain on the circulation forced by prescribed diabatic heating over the Amazon Basin. The behavior of the steady-state and the transient components of the response were analyzed separately in simulations with a forcing that rose slowly to a steady level and a forcing that peaked rapidly and then decayed to zero. The response in the case with no topography was compared with the results of previous studies with linear models. The near agreement suggests that linear models accurately describe both the steady and the transient response to realistic values of the heating in the absence of topography.

The principle effect of topography on the steady-state solution is to block low-level flow from the equatorial Pacific into the region of the heating. In the presence of topography the source of the low-level inflow switches to the equatorial Atlantic. As this flow impinges on the topography, it is deflected southward and is concentrated into a low-level jet identifiable in the model from just north of the equator down through the latitude of maximum heating at 11°S. A similar conclusion was drawn by Kleeman (1989) on the basis of the evolution of the transient solution over a 3-day time span. The pattern of downward vertical motion (Fig. 6b) suggests that the roots of the flow entering the steady-state jet lie in an overturning in the equatorial plane that is both shallow and of small zonal scale. Simulations done with various values of the coefficient of linear damping revealed that the zonal scale is smaller, the larger the damping. South of the latitude of maximum heating the jet turns rapidly westward and then northward around a cyclonic center situated at the eastern base of the topography. This description of the low-level response pattern is sensitive to the presence of a basic-state flow insofar as a relatively weak flow of 1.5 m s^{-1} from the west appears to be sufficient to eliminate the inflow from the equatorial Atlantic.

The steady-state simulation also indicates that topography engenders a small region of strong descent on its eastern equatorial slope. Inspection of the horizontal flow pattern on the lowest σ surface (Fig. 5a) suggests that the descent involves some mixture of air coming over the topography from the Pacific together with air flowing westward from the equatorial Atlantic that moves up the topographic ridge and then sinks back to flow into the low-level jet. The dynamics of this isolated region of strong descent are not clear. Since the equation that yields ω in the σ-coordinate formulation contains the difference of two relatively large terms, there is the possibility of truncation error. To test this hypothesis, the simulation was repeated with the horizontal gridpoint spacing reduced by a factor of two from its standard value of 3.75°. This and other features of the vertical motion field were little changed.

Simulations with the transient heat source in the presence of topography are in agreement with results reported by Kleeman (1989). The essential points of his findings were that the topography scatters the transient response incident from the source region to the east of it into a reflected baroclinic Kelvin wave packet and a transmitted, barotropic Rossby wave packet. We considered the effects of three forms of topography on the nature of the reflected Kelvin wave response. In the case of extremely narrow (knife-edge) topography of 4 km in altitude, the reflected Kelvin wave packet has the vertical structure of a single vertical normal mode. The amplitude of the reflected wave packet is about 30 percent of the direct Kelvin wave packet that emanates from the heat source. Topography of the same height, but of finite width, produces a reflected component of the same amplitude and a more complicated vertical structure. The more complicated vertical structure seems to be the only difference in the response to knife-edge versus finite-width topography. Reduction of the height of finite-width topography by a factor of two reduces the amplitude of the reflected wave by the same factor.

Our analysis of the transmitted component of the response in the presence of topography lends some support to the interpretation (Kleeman 1989) that the relative maximum in external-mode amplitude over the eastern Pacific identified in the observational study by Silva Dias and Bonatti (1985) is the result of scattering into the external mode by the Andes chain of energy incident from the heating region over the Amazon Basin. The 10 m amplitude that is found in the case of topography of 4 km altitude is, however, about half of that found in the observational study. In the case of the smooth topography of 2 km altitude, the amplitude of the barotropic component over the eastern Pacific is so small as to be difficult to estimate by this technique, but is certainly no more than a few meters. This topography is certainly closer to reality than topography of 4 km amplitude. There thus remains a substantial discrepancy in amplitude between the observed barotropic feature over the eastern Pacific and simulation of the effect on this region of distant heating to the east of the Andes.

Acknowledgments. This research was supported in part by the National Science Foundation under Grants ATM-8715360 and ATM-8913279. The visit of Adilson Gandu was made possible by support from the Brazilian agency Coordenação de Aperfeiçoamento de Pessoal de Nivel Superior (CAPES).

REFERENCES

Arakawa, A., and V. R. Lamb, 1977: Computational design of the basic dynamical process of the University of California at Los Angeles general circulation model. Methods of Computational Physics, Vol. 17, Academic Press, 174–265.

Buchmann, J., P. L. Silva Dias and A. D. Moura, 1986: Transient convection over the Amazon Bolivia region and the dynamics of droughts over northeast Brazil. *Arch. Meteor. Geophys. Bioklim. Ser. A.,* **34,** 367–384.

DeMaria, M., 1985: Linear response of a stratified tropical atmosphere to convective forcing. *J. Atmos. Sci.,* **42,** 1944–1959.

Dickinson, R. E., 1984: Modeling evapotranspiration for three-dimensional global climate models. *Climate Processes and Climate Sensitivity. Geophys. Monogr.,* No. 29, J. E. Hansen and T. Takahashi, Eds., Amer. Geophys. Union, 58–72.

——, and A. Henderson-Sellers, 1988: Modelling tropical deforestation: A study of GCM land-surface parameterization. *Quart. J. Roy. Meteor. Soc.,* **114,** 439–462.

Gill, A. E., 1980: Some simple solutions for heat-induced tropical circulation. *Quart. J. Roy. Meteor. Soc.,* **106,** 447–462.

Horel, J. D., A. N. Hahmann and J. E. Geisler, 1989: An investigation of the annual cycle of convective activity over the tropical Americas. *J. Climate,* **2,** 1388–1403.

Kleeman, R., 1989: A modeling study of the effect of the Andes on the summertime circulation of tropical South America. *J. Atmos. Sci.,* **46,** 3344–3362.

Kreuels, R., K. Fraedrich and E. Ruprecht, 1975: An aerological climatology of South America. *Meteor. Rundsch.,* **28,** 17–24.

Nobre, C. A., P. Sellers, J. Shukla, J. Kinter and L. Marx, 1989: Amazon deforestation: A coupled biosphere–atmosphere GCM experiment. Extended Abstracts, *Third International Conference on Southern Hemisphere Meteorology and Oceanography,* Buenos Aires, Amer. Meteor. Soc., 66–69.

Orlansky, I., 1976: A simple boundary condition for unbounded hyperbolic flows. *J. Comput. Phys.,* **21,** 251–269.

Sellers, P., Y. Mintz, Y. C. Sud and A. Dalcher, 1986: A simple biosphere model (SiB) for use within general circulation models. *J. Atmos. Sci.,* **43,** 505–531.

Silva Dias, P. L., and J. P. Bonatti, 1985: A preliminary study of the observed vertical mode structure of the summer circulation over tropical South America. *Tellus,* **37A,** 185–195.

——, W. H. Schubert and M. DeMaria, 1983: Large-scale response of the tropical atmosphere to transient convection. *J. Atmos. Sci.,* **40,** 2689–2707.

Smith, R. B., 1979: Some aspects of the quasi-geostrophic flow over mountains. *J. Atmos. Sci.,* **36,** 2385–2393.

Virji, H., 1981: A preliminary study of summertime tropospheric circulation patterns over South America estimated from cloud winds. *Mon. Wea. Rev.,* **109,** 599–610.